



SYNTHESIS, ADMET, DOCKING AND MOLECULAR DYNAMICS OF NEW MOLECULES DERIVATIVES FROM 1,3,4-OXADIAZOLE AND 1,3,4-BISOXADIAZOLE: NEW COMPOUNDS AGAINST HIV

Assiya Atif^{1*}, Soukaina Zahm², Said Jebbari¹, Abouelhaoul El Alami¹, Fatima Youssoffi¹, Houssine Ait Sir¹, Said Kerraj² and Mohammed Salah³

Abstract

Our synthesis method for 1,3,4-oxadiazole derivatives, involving the condensation of hydrazide derivatives with carboxylic acids in the presence of phosphoryl trichloride, holds significance across diverse scientific domains. Structural confirmation of the synthesized compounds employs infrared spectroscopy (IR), proton nuclear magnetic resonance spectroscopy (¹H NMR), carbon nuclear magnetic resonance spectroscopy (¹³C NMR) and mass spectrometry (MS). In tandem with experimental techniques, our study includes ADMET studies (Absorption, Distribution, Metabolism, Excretion, and Toxicity), docking studies, and molecular dynamics simulations. These computational analyses offer valuable insights into the pharmacokinetic properties of the compounds, potential interactions with target molecules (e.g., enzymes or receptors), and their dynamic behavior. The integration of experimental synthesis and characterization with computational methodologies enhances our understanding of 1,3,4-oxadiazole and 1,3,4-bisoxadiazole derivatives. This combined approach contributes to the exploration of these compounds' potential applications in biological, pharmaceutical, and chemical contexts, facilitating the development of new compounds with desirable properties.

Keywords: Oxadiazole; Bisoxadiazole; ADMET; Docking; Molecular dynamics

¹Bioorganic Chemistry Team, Faculty of Science, Chouaib Doukkali University, P.O. Box 20, 24000 El Jadida, Morocco.

²Laboratory of Physical Chemistry of Materials, Faculty of Sciences Ben M'Sik, Hassan II University, P.O. Box 7955, Casablanca, Morocco.

³Molecular Modelling and Spectroscopy Research Team, Faculty of Science, Chouaib Doukkali University, P.O. Box 20, 24000 El Jadida, Morocco.

*Corresponding authors: Assiya Atif

*Email: assia.atif@gmail.com

DOI: 10.53555/ecb/2023.12.12.290

Introduction

Heterocycles represent a pivotal category within organic chemistry, holding paramount importance across diverse fields. In particular, the pharmaceutical and agrochemical industries heavily rely on heterocyclic compounds owing to their manifold biological activities and therapeutic potential. Among these, oxadiazole emerges as a particularly intriguing heterocyclic compound. The structure of 1,3,4-oxadiazole, featuring a five-membered cycle with one oxygen atom and two nitrogen atoms, embodies unique properties and reactivity patterns, rendering it attractive for various scientific applications. Its aromatic nature contributes to both stability and potential interactions with biological targets. A comprehensive understanding of the structure and properties of oxadiazole compounds, including 1,3,4-oxadiazole, is imperative for the design and development of novel compounds tailored for pharmaceutical, agrochemical, and industrial applications. The escalating interest and surge in patent applications involving oxadiazole compounds underscore their profound significance and potential transformative impact in the realm of chemistry (Fig. 1) [1].

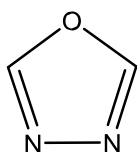
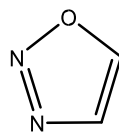
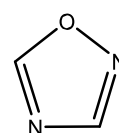


Fig. 1 : General structure of 1,3,4-oxadiazole.

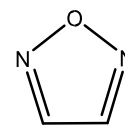
There are three other known isomers of oxadiazole (Fig.2), namely 1,2,3-oxadiazole; 1,2,4-oxadiazole, and 1,2,5-oxadiazole [2].



1,2,3-oxadiazole



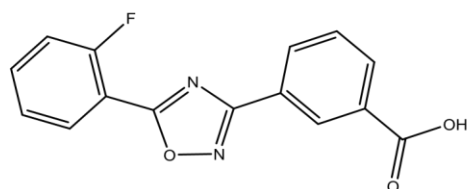
1,2,4-oxadiazole



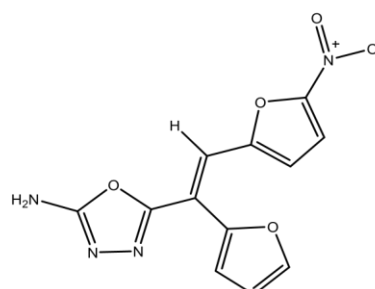
1,2,5-oxadiazole

Fig. 2 : General structure of oxadiazole isomers

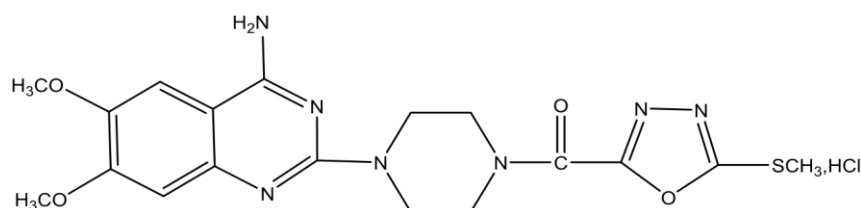
1,3,4-oxadiazole-containing compounds have successfully transitioned into commercial drug products, exemplifying their pivotal role in drug discovery and development (refer to Fig. 3). Noteworthy examples include Ataluren and Furamizole. Ataluren, an orally administered medication, has gained approval for treating a specific type of cystic fibrosis resulting from a distinct genetic mutation. Functioning as a "readthrough" agent, Ataluren facilitates ribosomes in reading through premature stop codons in messenger RNA, thereby enabling the synthesis of functional proteins. The presence of a 1,3,4-oxadiazole moiety in Ataluren is a critical structural element contributing to its pharmacological activity [3]. Furamizole, on the other hand, exhibits potent antibacterial properties, particularly against *Helicobacter pylori*, a bacterium linked to gastric ulcers and other gastrointestinal conditions. The antimicrobial efficacy of Furamizole is attributed to its 1,3,4-oxadiazole core, and it has been explored for its potential as an anti-ulcer agent [4]. These examples underscore the versatility and therapeutic potential of 1,3,4-oxadiazole-containing compounds in the pharmaceutical landscape.



3-(5-(2-fluorophenyl)-1,2,4-oxadiazol-3-yl)benzoic acid



(E)-5-(1-(furan-2-yl)-2-(5-nitrofuran-2-yl)vinyl)-1,3,4-oxadiazol-2-amine



(5-(λ²-chloranyl)-1,3,4-oxadiazol-2-yl)(4-(4-amino-6,7-dimethoxyquinazolin-2-yl)piperazin-1-yl)methanone

Fig. 3: Commercially available drugs which contain oxadiazole nucleus

The diverse array of Activity of 1,3,4-oxadiazole derivatives positions them as promising candidates across various domains. As documented in the literature [5-19], these derivatives have demonstrated antifungal, antiproliferative, anticancer, and anti-inflammatory properties. Their versatility extends to applications as muscle relaxants, tranquillizers, cathepsin K inhibitors, angiogenesis inhibitors, HIV integrase inhibitors, and tyrosinase inhibitors in medicinal chemistry. Moreover, their utility as corrosion inhibitors, ability to form metal complexes, and involvement in polymer formation broaden their scope into materials science and industrial chemistry. Synthesis of series 1,3,4-oxadiazoles and 1,3,4-bisoxadiazole compounds is of particular interest. Characterizing their structures using spectroscopic techniques such as infrared spectroscopy (IR), proton nuclear magnetic resonance spectroscopy (^1H NMR), carbon nuclear magnetic resonance spectroscopy (^{13}C NMR) and mass spectrometry (MS) offers insights into their chemical properties and confirms molecular structures. Furthermore, comprehensive ADMET studies, docking studies, and molecular dynamics simulations aim to unveil pharmacokinetic properties, potential interactions with target molecules, and their dynamic behavior. These computational analyses aid in predicting drug-likeness, optimizing properties, and guiding further design and development efforts. Through the integration of experimental characterization with computational studies, this paper endeavors to explore structure-activity relationships and potential applications of the synthesized 1,3,4-oxadiazole and 1,3,4-bisoxadiazole compounds. Such an integrated approach holds the potential to contribute to the development of novel.

I. Experimental

1. General Informations

The progress of the reactions is monitored by thin layer chromatography (TLC) on aluminum foils coated with Merck 60 F254 silica gel (thickness 0.2 mm). The revelation is carried out under a UV-Visible lamp (at 254 and 365 nm). The melting points of synthesized compounds were also determined by a Köfler bench and are not corrected in degrees Celsius. FTIR spectra are recorded on a SHIMADZU FT-IR 8400S spectrometer with a Smart iTR accessory and attenuated with total reflection (ATR) crystal diamond in the range of (500-4000 cm^{-1}). The ^1H NMR and ^{13}C NMR spectra were recorded on a Fourier transform apparatus JNM-ECZ500/S1 FT

NMR SYSTEM (JEOL) (500 MHz for the proton and 125 MHz for carbon-13) of the National Center for Scientific Research and Technical (CNRST) in Rabat. The spectra are referenced to the solvent in which they are made (^1H NMR: DMSO- d_6 = 2.5 ppm and ^{13}C NMR: DMSO- d_6 = 39.7 ppm). High-resolution mass spectrometry is carried out on an Ultimate 3000-Exactive plus THERMO quadrupole-Orbitrap type device, equipped with a collision cell from the National Center for Scientific and Technical Research (CNRST) in Rabat.

2. Synthesis of 2-methyl-1H-benzimidazole carboxylic acid [20-21] (1)

Glacial acetic acid (60 mmol) was added to a solution of 3,4-diaminobenzoic acid (40 mmol) in concentrated hydrochloric acid (30 ml). The reaction mixture was refluxed for 6 hours. After cooling, adjust the reaction medium to pH=4 with 25% ammoniac, filter the formed precipitate and recrystallize it in ethanol to obtain a brown powder. **Yield:** 85%, **m.p:** >300°C

3. Synthesis of ethyl 2-methyl-1H-benzimidazole-5-carboxylate [22] (2)

In order to prepare compound (2), (7mmols) of compound (1) was placed in absolute ethanol (30ml), then (8ml) of thionyl chloride was added at 0°C, and the reaction mixture was refluxed for 24 hours. After stopping the reaction, the mixture was neutralised to pH = 7 with a sodium bicarbonate NaHCO_3 solution 10%. The precipitate formed was filtered and recrystallised in ethanol as a buff powder. **Yield:** 79%, **m.p:** 170°C

4. Synthesis of 2-methyl-1H-benzimidazole-5-carbohydrazide (3)

To prepare compound (3), 7 mmol of compound (2) and hydrazine hydrate (10 mL) were stirred at room temperature for 18 hours. The reaction mixture was then concentrated and triturated with methanol several times to remove excess hydrazine hydrate. The solid was recrystallized in ethanol and obtained as a brown powder. **Yield:** 80%, **m.p:** 262°C

5. General synthesis of oxadiazole derivatives [23] (5)

3 mmols of the acid (4) were dissolved in (15ml) of phosphoryl trichloride, 3 mmols of 2-methyl-1Hbenzimidazole-5-carbohydrazide (3) were added to this solution, the reaction mixture was heated at reflux for 6 h. After stopping the reaction, the mixture was neutralised with

ammoniac 25% to pH=7, the precipitate formed was filtered and recrystallised in ethanol.

(5-1): 2-methyl-5-(2-methyl-1H-benzimidazol-5-yl)-1,3,4-oxadiazole

Yield: 73%, **m.p.:**224°C, ¹H NMR (500MHz/DMSO-d₆, ppm): 2.48(s,3H,CH₃), 2.52(s,3H,CH₃), 12.50(s,1H, NH), 7.71(d,1H, aromatic CH), 7.88(d,1H, aromatic CH), 8.00 (s,1H, aromatic CH) , ¹³C NMR (125MHz/DMSO-d₆, ppm): 161.46, 161.04, 160.60, 136.44, 134.41, 128.37, 124.53, 120.80, 117.53, 19.84,19.10, **IR (cm⁻¹):** 3149 νN-H, 1633 νC=N, 1286 νC-H, **MS (ESI):** m/z = 215[M+H]⁺.

(5-2): 2-(2-methyl-1H-benzimidazol-5-yl)-5-phenyl-1,3,4-oxadiazole

Yield: 57%, **m.p.:**130°C, ¹H NMR (500MHz/DMSO-d₆, ppm): 2.51(s,3H,CH₃), 7.23(d,1H, aromatic CH),7.38(dd,1H, aromatic CH), 7.46(dd,1H, aromatic CH), 7.56(dd,1H, aromatic CH), 7.72(d,1H, aromatic CH), 7.88(d,1H, aromatic CH), 8.05(s,1H, aromatic CH), 8.16(d,1H, aromatic CH), 10.25(s,1H,NH), ¹³C NMR (125MHz/DMSO-d₆, ppm): 161.46, 161.04, 160.60, 136.44, 134.41, 132.98, 132.44, 128.37, 126.44, 124.53,120.80, 117.53, 116.12, 115.51, 114.79, 19.84, **IR (cm⁻¹):** 3128 νN-H,1631 νC=N, 1288 νC-H ,**MS (ESI):** m/z = 277[M+H]⁺

(5-3): 2-(5-(2-methyl-1H-benzimidazol-5-yl)-1,3,4-oxadiazol-2-yl)aniline

Yield: 89%, **m.p.:**>300°C, ¹H NMR (500MHz/DMSO-d₆,ppm): 2.47(s,3H,CH₃), 6.75(s,2H,NH₂), 7.26(d,1H, aromatic CH), 7.38(dd,1H, aromatic CH), 7.47(d,1H, aromatic CH), 7.55(dd,1H, aromatic CH), 7.70(s,1H, aromatic CH), 7.81(d,1H, aromatic CH),8.05(d,1H, aromatic CH), 10.26(s,1H,NH), ¹³C NMR (125MHz/DMSO-d₆, ppm): 161.46, 161.04, 160.60,136.44, 134.41, 132.98, 132.44, 128.37, 126.44, 124.53, 120.80, 117.53, 116.12, 115.51, 114.79, 19.84, **IR (cm⁻¹):** 3408-3314 νNH₂, 3188 νN-H, 1640 νC=N, 1274 νC-H,**MS (ESI):** m/z = 292[M+H]⁺

(5-4):2-(2-methyl-1H-benzimidazol-5-yl)-5-(2-(trifluorométhyl)-1H-benzimidazol-5-yl)-1,3,4-oxadiazole

Yield: 44%, **m.p.:** 244°C, ¹H NMR (500MHz/DMSOd₆,ppm):2.52(s,3H,CH₃),7.87(s, 1H, aromatic CH),7.88(1H,d, aromatic CH),7.90(1H,d, aromatic CH),8.12(1H,s, aromatic CH),8.18(1H,d, aromatic CH), 8.20(d,1H,

aromatic CH), 10.47(s,1H, NH), 10.58(s,1H, NH), ¹³C NMR (125MHz/DMSO-d₆, ppm): 162.86, 161.46, 161.04, 160.60, 136.44, 124.41, 132.44, 128.37, 126.54, 124.53, 120.80, 117.53, 116.84, 116.41, 116.12,115.51, 115.32, 19.84, **IR (cm⁻¹):** 3178 νN-H, 1629 νC=N,1059 νC-F,**MS (ESI):** m/z = 385[M+H]⁺

(5-5): 2,5-bis(2-methyl-1H-benzimidazol-5-yl)-1,3,4-oxadiazole

Yield: 63%, **m.p.:**>300°C, ¹H NMR (500MHz/DMSO-d₆,ppm): 2.51(s,3H,CH₃), 7.58(s,1H, aromatic CH) 7.70(d,1H, aromatic CH), 7.88(d,1H, aromatic CH), 12.56(s,1H,NH), ¹³C NMR (125MHz/DMSO-d₆, ppm): 165.51, 164.56, 164.14, 132.39, 129.93, 127.11, 124.04, 120.81, 116.90, 15.16,**IR (cm⁻¹):** 3121 νN-H, 1633 νC=N, 1293 νC-H ,**MS (ESI):** m/z = 331[M+H]⁺

6. Synthesis of diethyl oxalate [24] (7)

Oxalic acid (6) is dissolved (7 mmols) in absolute ethanol (15 ml), then a few sulfuric acid droplets are added. Six hours were spent refluxing the mixture, then neutralised with sodium bicarbonate 10% to pH = 7, followed by liquid-liquid extraction with ethyl acetate, evaporation of which yielded the ester (7) in liquid form. **Yield:** 69%, **m.p.:** - 41°C

7. Synthesis of oxalohydrazide [25] (8)

Dissolve (5 mmols) of ester (7) in (30 ml) of absolute ethanol, then add (5 ml) of hydrazine hydrate. The concoction was heated under reflux for 10 hours. After evaporating the ethanol, we were able to recover the solid obtained. **Yield:** 75%, **m.p.:** 242 °C

8. General snthesis of bisoxadiazole derivatives [23] (10)

To a solution of (6mmols) carboxylic acid (9) in (20ml) phosphorylchloride, after adding (3 mmol) of oxalohydrazide, the liquid refluxed for 6 hours. After cooling, the mixture was neutralised with ammoniac 25% to pH = 7, the precipitate formed was filtered and recrystallised in ethanol.

(10-1) : 5,5'-bis(2-methyl-1H-benzimidazol-5-yl)-2,2'-bis(1,3,4-oxadiazole)

Yield: 57%,**m.p. :**>300°C ,¹H NMR (DMSO-d₆,ppm): 2.52(s,3H,CH₃), 7.71(d,1H, aromatic CH), 7.89(d,1H, aromatic CH),8. 00(s,1H, aromatic CH), 12.46(s,1H, NH), ¹³C NMR (125MHz/DMSO-d₆, ppm): 161.46, 161.04, 160.60, 136.44, 134.41, 130.54, 127.70, 124.53,

121.62, 49.84, **IR** (cm^{-1}): 1632 $\nu_{\text{C}=\text{N}}$, 1291 $\nu_{\text{C}-\text{H}}$, 3223 $\nu_{\text{N}-\text{H}}$, **MS(ESI)**: $m/z = 399$ $[\text{M}+\text{H}]^+$

(10-2): 2,2'-([2,2'-bis(1,3,4-oxadiazole)]-5,5'-diyl)diphenol

Yield: 82%, **m.p** : $>300^\circ\text{C}$, **^1H NMR (DMSO- d_6 , ppm):** 7.35(d,1H, aromatic CH), 7.39(dd,1H, aromatic CH), 7.52(d,1H, aromatic CH), 7.83(dd,1H, aromatic CH), 10.15(s,1H, OH), **^{13}C NMR (125MHz/DMSO- d_6 , ppm):** 164.46, 163.59, 148.29, 132.89, 128.28, 116.74, 116.11, 104.75, **IR** (cm^{-1}): 3124 $\nu_{\text{O}-\text{H}}$ 1634 $\nu_{\text{C}=\text{N}}$, 1133 $\nu_{\text{C}-\text{O}-\text{C}}$, **MS(ESI)**: $m/z = 323$ $[\text{M}+\text{H}]^+$

(10-3) : 4,4'-([2,2'-bis(1,3,4-oxadiazole)]-5,5'-diyl)bis(benzene-1,2-diamine)

Yield: 65% , **m.p** : 240°C , **^1H NMR (DMSO- d_6 , ppm):** 6.60(s,2H, NH_2), 6.63(s,2H, NH_2), 7.16(s,1H, aromatic CH), 7.63(d,1H, aromatic CH), 7.94(d,1H, aromatic CH), **^{13}C NMR (125MHz/DMSO- d_6 , ppm):** 161.46, 161.04, 136.44, 134.41, 130.54, 127.70, 124.53, 121.62, **IR** (cm^{-1}): 1625 $\nu_{\text{C}=\text{N}}$, 3025-3125 ν_{NH_2} , **MS(ESI)**: $m/z = 351$ $[\text{M}+\text{H}]^+$

(10-4): 5,5'-bis(4-methoxyphenyl)-2,2'-bis(1,3,4-oxadiazole)

Yield: 91%, **m.p** : 246°C , **^1H NMR (DMSO- d_6 , ppm):** 4.12(s,3H, OCH_3), 7.00(d,1H, aromatic CH), 7.14(d,1H, aromatic CH), 7.61(d,1H, aromatic CH), 7.93(d,1H, aromatic CH), **^{13}C NMR (125MHz/DMSO- d_6 , ppm):** 162.32, 162.02, 137.56, 130.30, 129.65, 116.05, 113.84, 103.52, 68.99, **IR** (cm^{-1}): 1667 $\nu_{\text{C}=\text{N}}$, 1287 $\nu_{\text{C}-\text{O}}$, **MS(ESI)**: $m/z = 351$ $[\text{M}+\text{H}]^+$

(10-5): 6,6'-([2,2'-bi(1,3,4-oxadiazole)]-5,5'-diyl)bis(3-chloroaniline)

Yield: 78%, **m.p** : $>300^\circ\text{C}$, **^1H NMR (DMSO- d_6 , ppm):** 6.60(s,2H, NH_2), 7.16(s,1H, aromatic CH), 7.63(d,1H, aromatic CH), 7.87(d,1H, aromatic CH), **^{13}C NMR (125MHz/DMSO- d_6 , ppm):** 161.46, 161.04, 136.44, 132.98, 128.79, 120.66, 117.53, 114.79, **IR** (cm^{-1}): 1664 $\nu_{\text{C}=\text{N}}$, 3125-3202 ν_{NH_2} , **MS(ESI)**: $m/z = 389$ $[\text{M}+\text{H}]^+$

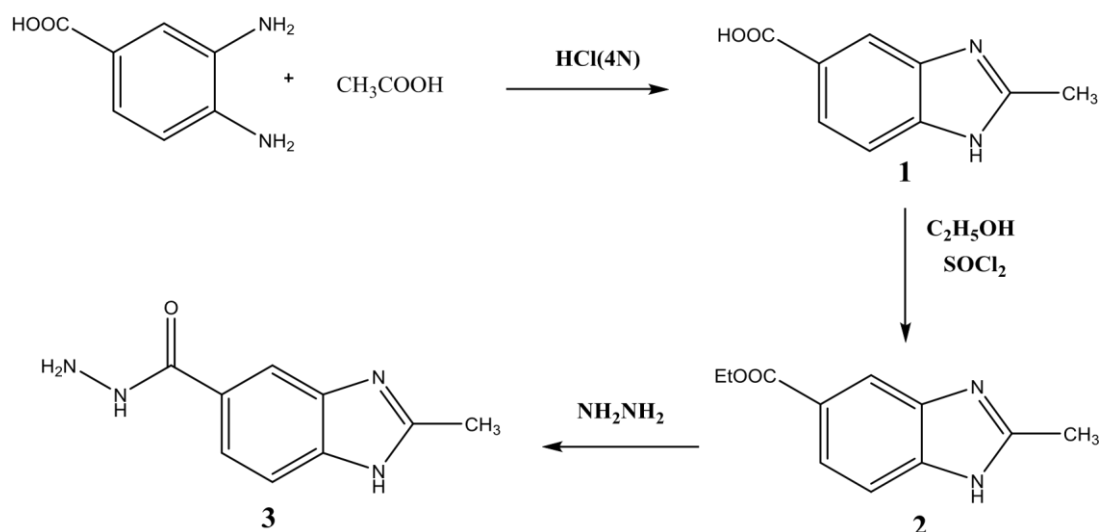
(10-6): 2,2'-([2,2'-bi(1,3,4-oxadiazole)]-5,5'-diyl)dianiline

Yield: 95% , **m.p** : $>300^\circ\text{C}$, **^1H NMR (DMSO- d_6 , ppm):** 6.41(s,2H, NH_2), 7.38(dd,1H, aromatic CH), 7.47(dd,1H, aromatic CH), 7.55(d,1H, aromatic CH), 7.78(d,1H, aromatic CH), **^{13}C NMR (125MHz/DMSO- d_6 , ppm):** 161.46, 161.04, 136.44, 134.41, 130.54, 127.70, 124.53, 121.62, **IR** (cm^{-1}): 1667 $\nu_{\text{C}=\text{N}}$, 3101-3156 ν_{NH_2} , **MS(ESI)**: $m/z = 321$ $[\text{M}+\text{H}]^+$

II. Results and discussion

1. synthesis of oxadiazoles

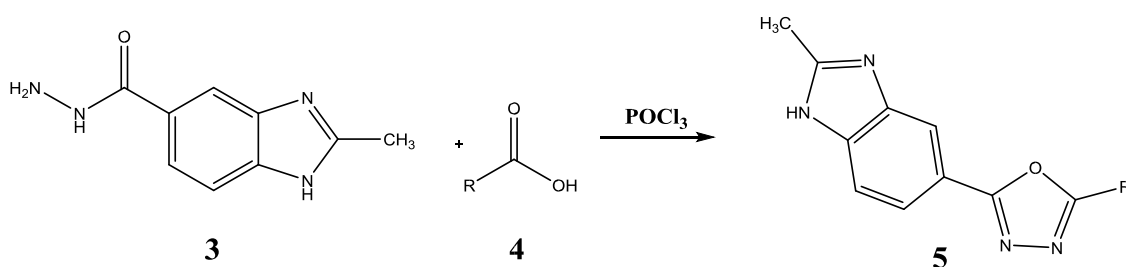
By employing the Phillips method [20][21] to condense 3,4-diaminobenzoic acid (OPDA) with acetic acid in hydrochloric acid, 2-Methyl-1H-benzimidazole-5-carboxylic acid (1) was produced in good yields [26][27]. The reaction between (1) and (2) produced the ester (2), which then reacted with an excess of hydrazine hydrate to form the acid hydrazide [28] (3). The esterification of (1) was performed in ethanol with thionyl chloride present.



Scheme 1: Synthesis of 2-methyl-1H-benzimidazole-5-carbohydrazide (3)

Various methods of accessing oxadiazole have been described in the literature [29], but in our work we reacted acid hydrazide (3) with

carboxylic acid derivatives (4) in the presence of phosphoryl trichloride under reflux to give oxadiazole derivatives (5).



Scheme 2: Synthesis of 1,3,4-oxadiazole derivatives (5)

2-methyl-5-(2-methyl-1H-benzimidazol-5-yl)-1,3,4-oxadiazole

The structure of 2-methyl-5-(2-methyl-1H-benzimidazol-5-yl)-1,3,4-oxadiazole was characterized and confirmed using IR, $^1\text{H-NMR}$, $^{13}\text{C-NMR}$ and mass spectrometry spectral data. The IR(ATR) spectrum shows in particular an absorption band at 1633 cm^{-1} attributed to the stretching vibration ($-\text{C}=\text{N}$) of the imine, a band at 1286 cm^{-1} corresponds to ($-\text{CH}$) methyl and a band at 3149 cm^{-1} for (N-H) imidazole. The ^1H NMR analysis of the isolated compound reveals the presence of two signals at 2.48 ppm and 2.52 ppm corresponding to the two methyl protons linked to benzimidazole and oxadiazole

respectively, this spectrum presents masses at 7.71, 7.88 and 8.00 ppm corresponding to aromatic protons, as well as a deshielded singlet at 12.50 ppm of imidazole nitrogen. The ^{13}C NMR spectrum of the compound highlights two signals 19.10 ppm and 19.84 ppm attributable to the methyl group carbon linked to benzimidazole and oxadiazole respectively, signals at 117.53, 120.80, 124.53, 128.37, 134.41 and 136.44 ppm due to aromatic carbons, as well as three signals at 160.60, 161.04 and 161.46 ppm corresponding to $\text{C}=\text{N}$ bonds. And finally, the mass spectrum of our product, taken in (ESI) indicates the presence of a molecular peak at the molecular ion $m/z = 215$ $[\text{M}+\text{H}]^+$.

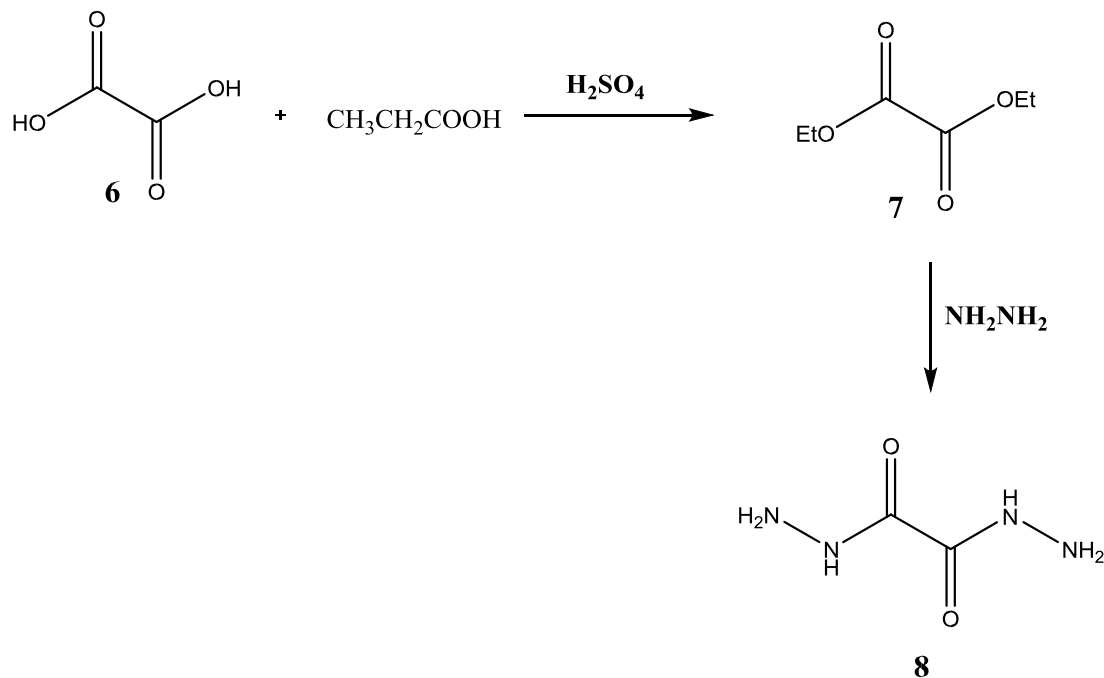
Table 1: derivatives compounds of 1,3,4-Oxadiazole

N°	Acid	compound	m.p	M	Yield
5-1			224 °C	214 g/mol	73%
5-2			130 °C	276 g/mol	57%
5-3			>300 °C	291 g/mol	89%
5-4			244 °C	384 g/mol	44%
5-5			>300 °C	330 g/mol	63%

2. Synthesis of bisoxadiazoles

Sulfuric acid was added to ethanol during the esterification process of (6) to produce ester (7).

The action of hydrazine hydrate on (7) leads to the bishydrazide (8).



Bisoxadiazole (10) was prepared from bishydrazide (8) and carboxylic acid derivatives (9) in the presence of phosphoryl trichloride.

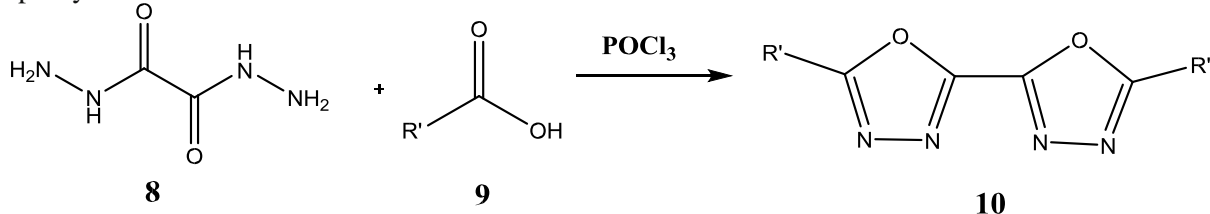
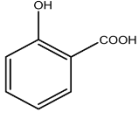
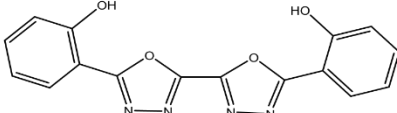
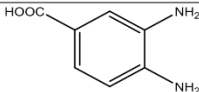
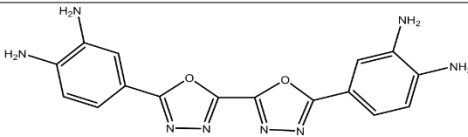
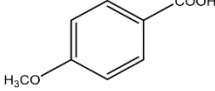
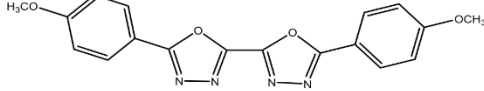
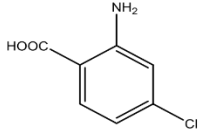
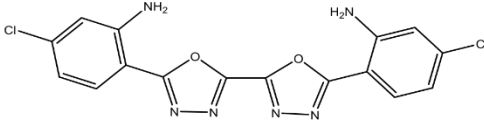
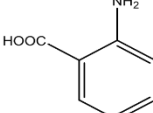
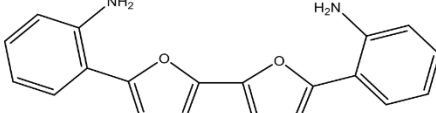


Table 2 : derivatives compounds of 1,3,4-Bisoxadiazole

N°	Acid	Compound	m.p	M (g/mol)	Yield
10-1			>300 °C	398	57 %

10-2			>300 °C	322	82 %
10-3			240 °C	318	65 %
10-4			246 °C	350	91 %
10-5			>300 °C	388	78 %
10-6			>300 °C	320	95 %

Synthesis of 5,5'-bis(2-methyl-1H-benzimidazol-5-yl)-2,2'-bis(1,3,4-oxadiazole)

Spectral analyzes of ^1H NMR, ^{13}C NMR, IR and mass spectrometry, as well as the comparison of its physical characteristics with those of a reference sample, allowed us to identify the structure of 5,5'-bis(2-methyl-1H-benzimidazol-5-yl)-2,2'-bis(1,3,4-oxadiazole). An absorption band at 1632 cm^{-1} in the IR(ATR) spectrum is attributed to the imine's ($-\text{C}=\text{N}$) stretching vibration. a band at 1291 cm^{-1} corresponds to ($-\text{CH}$) methyl and a band at 3223 cm^{-1} corresponds to ($-\text{N}-\text{H}$) benzimidazole. The ^1H NMR spectrum presents a singlet at 2.52 ppm relating to the methyl proton, masses at 7.71 ppm, 7.89 ppm and 8.00 ppm attributable to aromatic protons and the signal from the amine group linked to benzimidazole is observed at 12.46 ppm. In ^{13}C NMR, we note the presence of three signals at 161.46, 161.04 and 160.60 ppm attributable to the $\text{C}=\text{N}$ bonds, and signals at 136.44, 134.41, 130.54, 127.70, 124.53 and 121.62 ppm corresponding to the carbons of the benzene ring and the existence of a signal at 19.84 ppm due to the methyl group linked to benzimidazole. And finally, the mass spectrum of our product, taken in (ESI) indicates the presence of a molecular peak at $m/z = 399$ $[\text{M}+\text{H}]^+$.

III. ADMET, Docking and Molecular Dynamics

1. Molecular Docking Analysis

Molecular docking studies were carried out with the Maestro 13.4 software (Schrodinger 2022-4) to elucidate the interaction modes of the studied compounds (Table 3) with the HIV protein. The process involved several key steps:

Ligand Preparation:

A total of eleven ligands were prepared using Maestro 13.4's Ligprep wizard (Schrodinger 2022). In this phase, conflicts between bond length and angle were resolved, hydrogen atoms were added from 2D representations, and ligand structures were transformed into 3D. It was done to minimize and apply the OPLS force field 2005. The specified chirality was preserved, along with other features like the ionization state.

Targeted Protein Preparation:

Using the Maestro 13.4 protein preparation wizard, the initial geometries of the HIV protein were created. These geometries were obtained from the RCSB data bank website (PDB code 5CON: crystal structure of wild-type HIV-1 protease in complex with GRL-015). Using the Protein Preparation Wizard for pre-processing, refining, and reduction were noteworthy steps. Charge adjustments, bond order assignments, disulfide bond repairs, neutralization of side chains that were not close to the binding cavity, and zero-order bonds for metals were among the corrections made. Amino acid defects were fixed, hydroxyl groups and water molecules were

rearranged, and hydrogen atoms were added. After testing and modification, the chosen protein was subjected to restricted minimization in order to improve its structure.

Protein Site Mapping:

Following the preparation of the HIV protein, the Site Map was employed to identify and analyze binding sites based on protein size, functionality, and solvent exposure. The Site Score was utilized to assess the propensity of a site for ligand binding, ranking possible binding sites for pharmaceutical relevance.

Receptor Grid Generation:

Using the Site Map and a high site score, Glide molecular docking found the active site receptor grid. Next, ligands were inserted into the X-ray crystal structure of the protein to enable interactions in different conformations. During this phase, sites, limits, rotatable groups, and excluded volumes were implemented.

Molecular Docking Performance:

The three precision modes used for docking were HTVS (High Throughput Virtual Screening), SP (Standard Precision), and XP (Extra Precision). This was done after the target protein's active site was grid-constructed and the ligand and protein were prepared. By computing binding energies (ligand-protein interaction energies) in kcal/mol, this thorough method assessed binding interactions between molecules. Internal energy, RMSD, desolvation energy, lipophilic interactions,

π stacking interactions, and H-bonding were among the parameters that were found.

Docking Score:

Results of ligand-protein interactions and docking scores were used to evaluate docking experiments. Notably, a low negative binding energy determined during docking suggested that the ligands and the chosen protein had a good affinity and constancy.

Results and discussions:

As shown in [Figure 4](#), the presence of particular substituted groups, heteroatoms, and the structural geometry of the protein itself may have a significant impact on the binding affinity of the studied compounds at the HIV protein's active site. An investigation into the binding modes to the HIV protein was done using a molecular docking study in order to clarify the function of these factors. [Table 3](#) displays the estimated binding energies of the stable complexes that were formed between the HIV protein and the ligands under study. Remarkably, the formed complexes exhibited notable negative binding energies ([Table 3](#)), indicating their potential as effective viral inhibitors. The range of binding energies for the stable complexes varies between -4.2 to -7.6 kcal ([Table 3](#)). According to the molecular docking results, compound 10-2 demonstrated a high affinity (-7.5 kcal/mol) to the HIV protein in Extra Precision mode (XP), while 10-3 exhibited a binding energy of -7.1 kcal/mol in Standard Precision mode. Further insights into the interactions are provided in [Table 4](#).

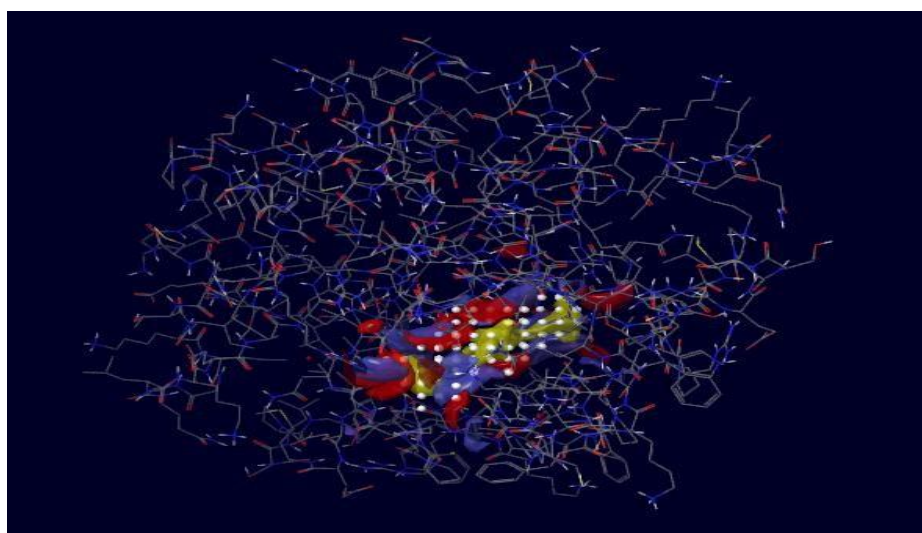
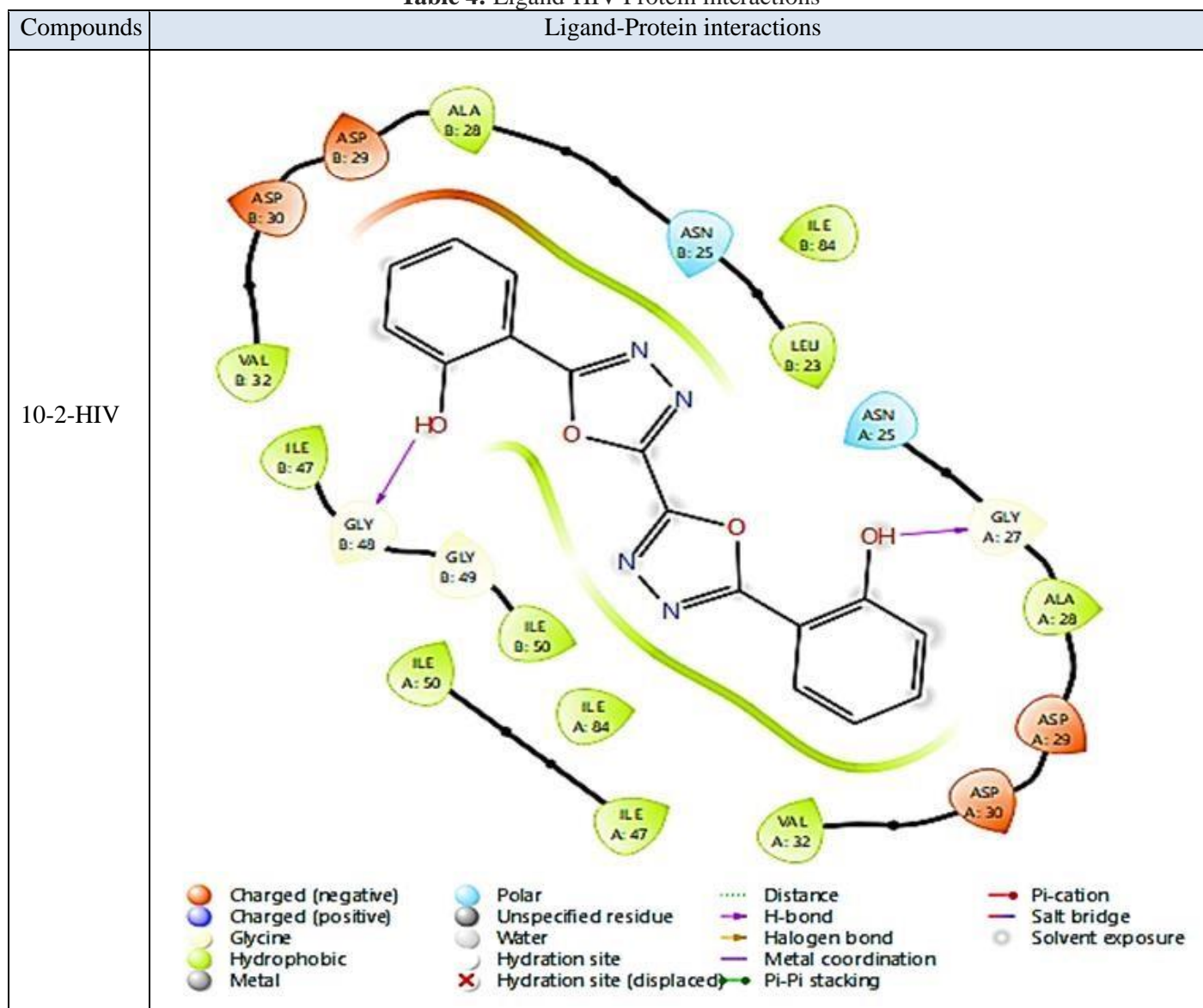


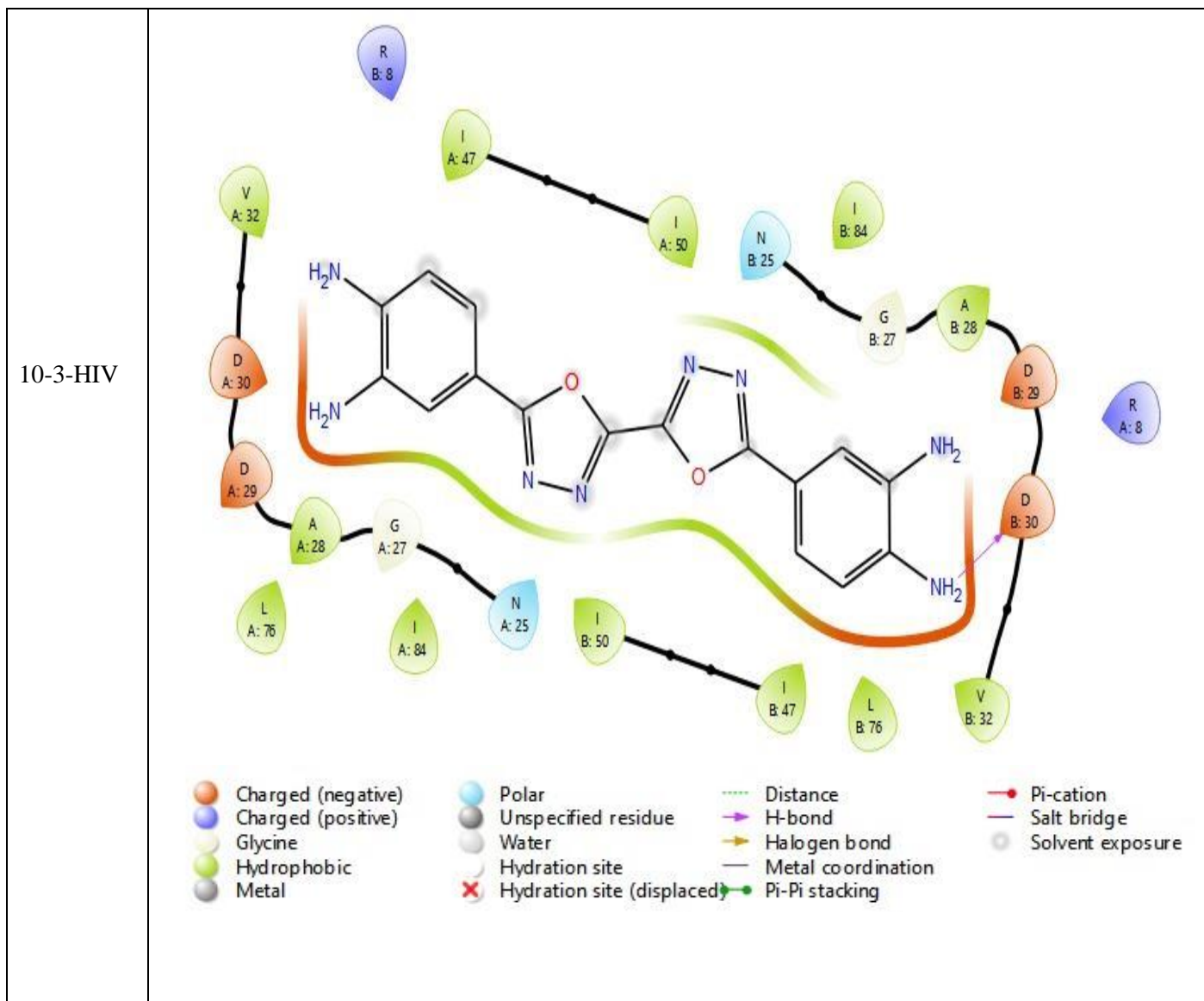
Fig. 4: the Active site on the prepared HIV protein

Table 3: estimated binding energies of the complex's ligand-HIV protein

	Compounds	Binding Energy		
		HTVS	SP	XP
X-ray crystal structure of wild type HIV-1 protease (PDB code 5CON)	5-1	-5.3	-5.3	-4.2
	5-2	-5	-5.6	-5.6
	5-3	-6.3	-6.6	-5.1
	5-4	-6	-7	-5.6
	5-5	-5.7	-7	-5.6
	10-1	-6.36	-6.3	-5.4
	10-2	-6.2	-7	-7.5
	10-3	-7.1	-7.1	-6
	10-4	-6	-6.6	-5.6
	10-5	-5.4	-6	-6
	10-6	-5.7	-6.4	-5.2

Table 4: Ligand-HIV Protein interactions





The active molecule within the compound, Ligand 10-2, demonstrated robust interactions at the HIV protein site. Two conventional hydrogen bonds were formed, exemplifying a strong affinity and stability of the ligand. Specifically, one hydrogen bond was established between the hydrogen atom of the OH group and the GLY A27 residue, while another formed between the hydrogen atom of the OH group and GLY B48. These interactions underscore the potent binding capabilities of Ligand 10-2 at the active site of the HIV protein. Conversely, the second novel compound, Ligand 10-3, exhibited a distinct interaction pattern. It formed a single hydrogen bond between the hydrogen atom of the NH group and the Asp B30 residue. Although fewer in number compared to Ligand 10-2, this hydrogen bond signifies a notable binding interaction between Ligand 10-3 and the HIV protein.

When considering binding affinity and interactions collectively, the docked Ligand 10-2

emerges as a stronger HIV inhibitor. This heightened inhibitory efficacy can be attributed to a combination of hydrophobic interactions and the presence of multiple conventional hydrogen bonds, highlighting its potential therapeutic significance in disrupting the HIV protein's functionality

2. Molecular Dynamic Study

The molecular dynamics simulation for the most potent compound, 10-3, in conjunction with the HIV protein 5CON, was successfully carried out using GROMACS, version 2023, released on February 6th, 2023. This comprehensive study aimed to elucidate the dynamic behavior of the ligand-protein complex under realistic conditions over a period of 50 nanoseconds. The simulation employed the CHARMM 27 force field, with the protein topology prepared using pdb2gmx and the ligand topology prepared via ProdDrg. The complex of ligand-protein was solvated in a cubic

unit cell, and a 0.15M concentration of NaCl salt was introduced. Subsequently, the system underwent relaxation through energy minimization, with fixed pressure set at 1 bar and temperature at 315 K. To assess the stability of the complex, various parameters were scrutinized, including the number of hydrogen bonds in the protein, gyration, solvent accessible surface area (SASA), Root Mean Square Deviation (RMSD),

and Root-Mean-Square Fluctuation (RMSF). The outcomes, as depicted in **Figures 5 to 9**, reveal a commendable stability exhibited by the complex throughout the 50 nanoseconds of dynamic simulation. This observation suggests that compound 10-3 forms and maintains a highly stable complex with the 5CON binding site, signifying its potential as a robust and enduring candidate for therapeutic intervention.

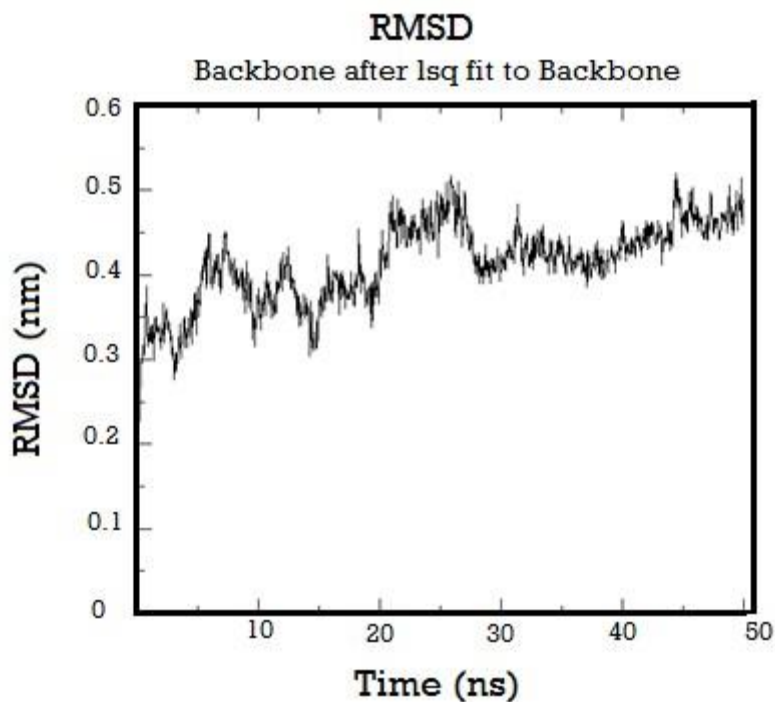


Fig. 5: RMSD (Root Mean Square Deviation)

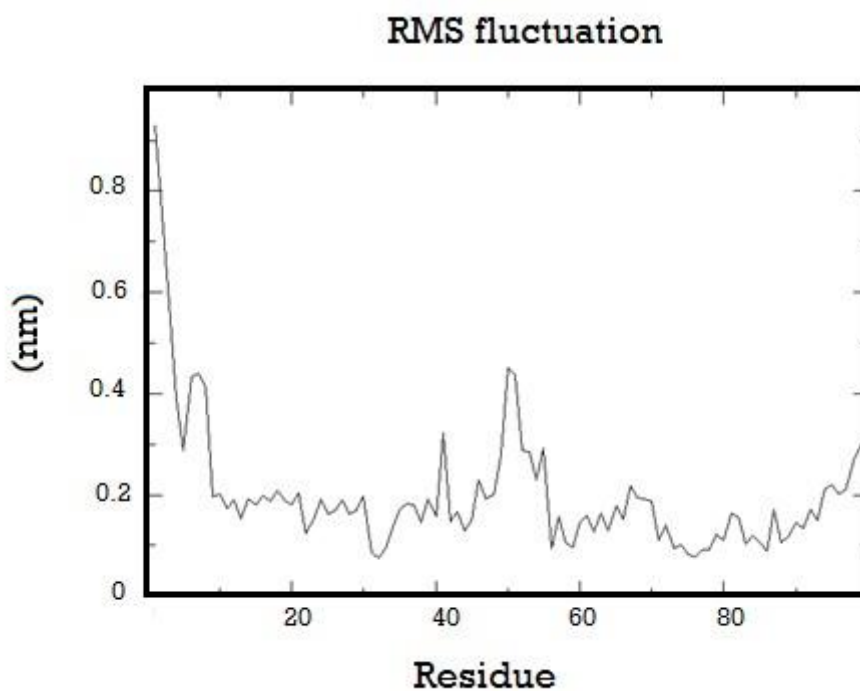


Fig. 6: RMSF (Root-Mean-Square Fluctuation)

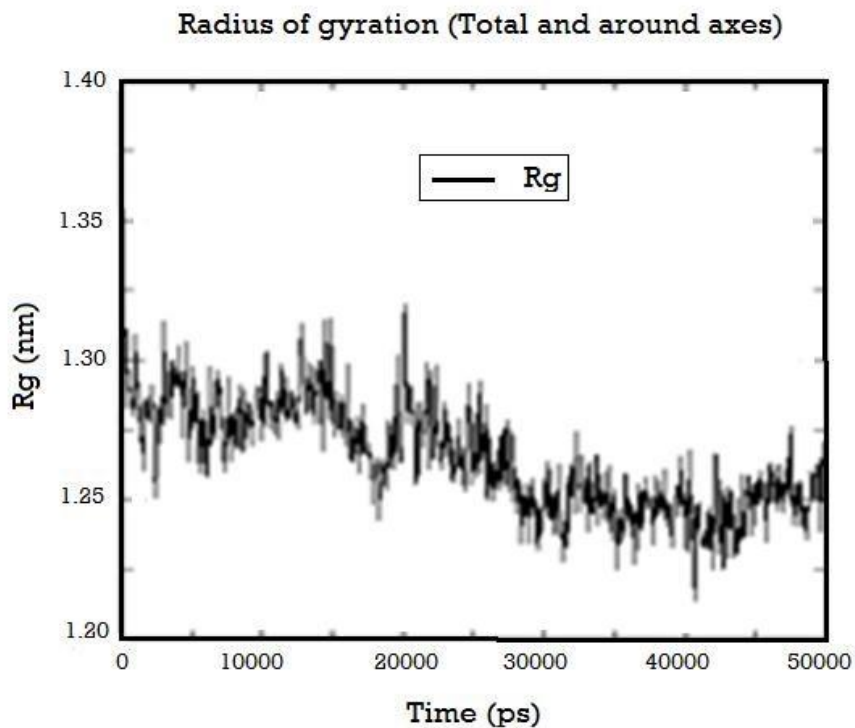


Fig. 7: Gyration raduis

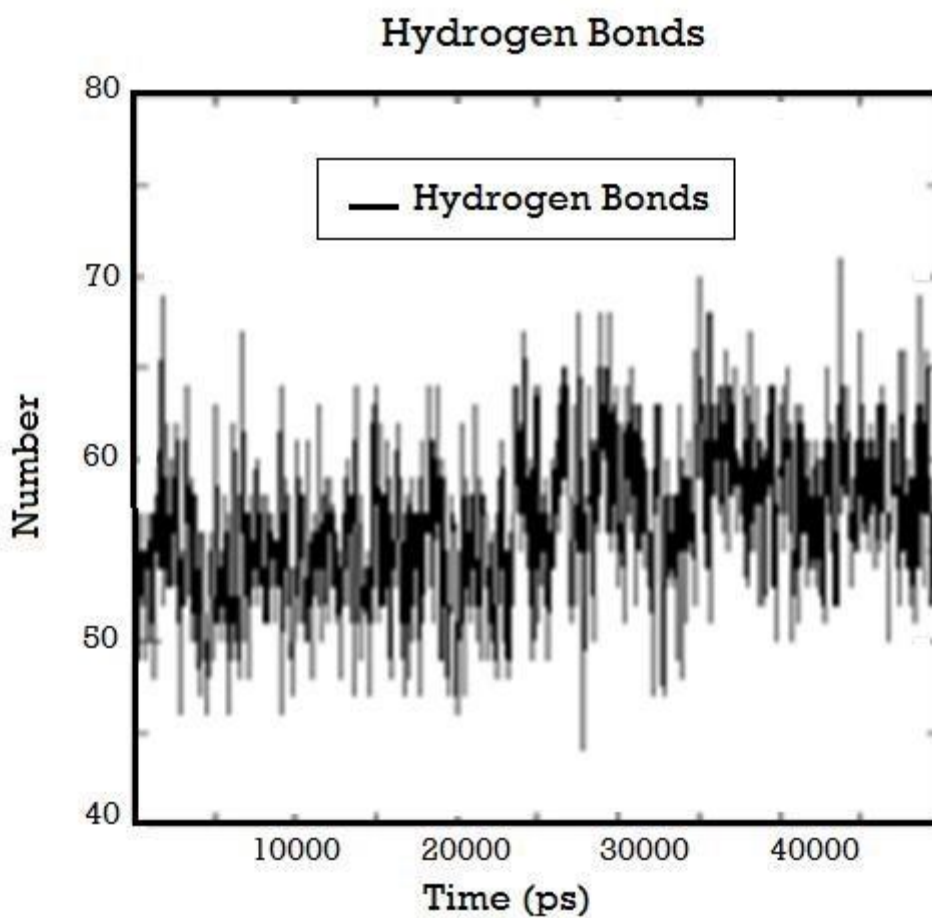


Fig. 8: Hydrogens bonds

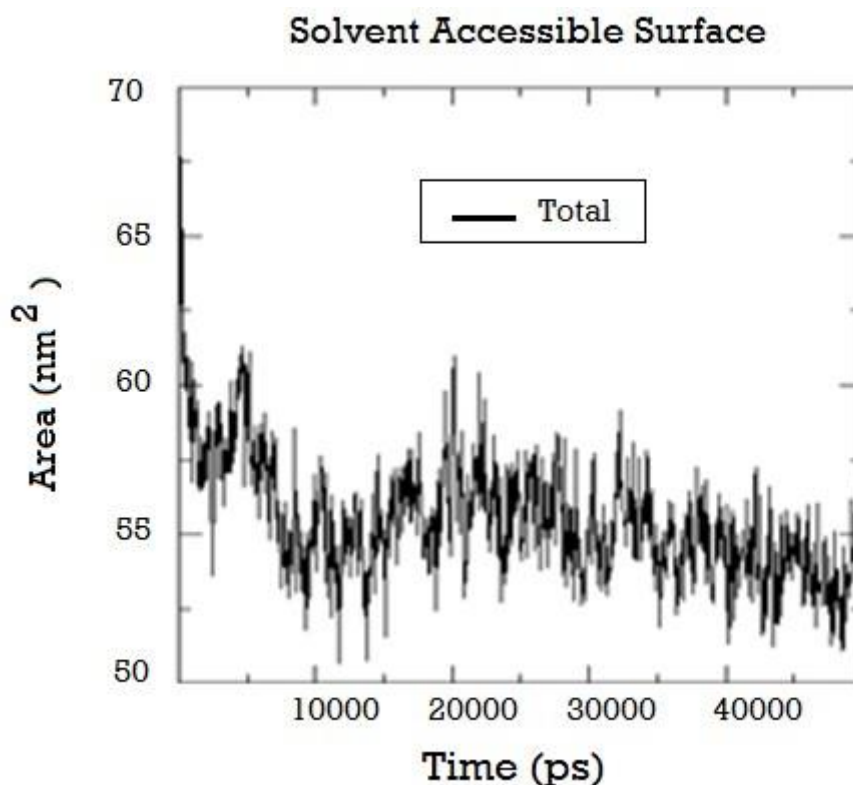


Fig. 9: SASA (Solvent accessible surface area)

3. ADMET and Druglikness Analysis

The study aimed to assess the pharmaceutical suitability of compounds 10-2 and 10-3 through comprehensive toxicity, ADME, and drug likeness evaluations. For toxicity, the Ames test and rodent carcinogenicity assay were employed, revealing a general absence of mutagenicity for all compounds. However, conflicting results emerged as TA100 and TA1535 showed positive mutagenic outcomes for compound 10-2. In terms of ADME, the PreADMET servers utilized in vitro methods, such as the CaCo₂ cell model and MDCK cell model, to predict absorption, distribution, metabolism, and excretion. Compound 10-2 exhibited high human intestinal absorption (HIA) values (88–100%), indicating favorable oral

absorption. Plasma protein binding analysis indicated strong binding for all compounds, notably 90.55% for 10-2. Additionally, compounds 10-2 and 10-3 displayed low central nervous system (CNS) absorption, suggesting advantageous blood-brain barrier properties. Despite generally negative mutagenicity results, the conflicting outcomes in TA100 and TA1535 for compound 10-2 warrant further scrutiny. These findings collectively imply potential oral administration benefits for compound 10-2, while emphasizing the need for nuanced interpretation and additional investigations to reconcile conflicting data and refine considerations for drug development.

Table 5: ADMET and Druglikness results of the three anti viral ligands

Compound 10-2: Toxicity, ADME and Druglikness		
Toxicity	ID	Value
	algae_at	0.0380161
	Ames_test	mutagen
	Carcino_Mouse	negative
	Carcino_Rat	positive
	daphnia_at	0.084217
	hERG_inhibition	medium_risk
	medaka_at	0.0136084
	minnow_at	0.0194188
	TA100_10RLI	positive
	TA100_NA	positive

	TA1535_10RLI	positive
	TA1535_NA	negative
ADME	ID	Value
	BBB	0.154517
	Buffer_solubility_mg_L	6085,73
	Caco2	12,7995
	CYP_2C19_inhibition	Inhibitor
	CYP_2C9_inhibition	Inhibitor
	CYP_2D6_inhibition	Non
	CYP_2D6_substrate	Non
	CYP_3A4_inhibition	Inhibitor
	CYP_3A4_substrate	Non
	HIA	89,15505
	MDCK	6,8047
	Pgp_inhibition	Non
	Plasma_Protein_Binding	90,55704
	Pure_water_solubility_mg_L	57,4212
	Skin_Permeability	-4,05272
	SKlogD_value	3,02618
	SKlogP_value	3,02618
	SKlogS_buffer	-1,72392
	SKlogS_pure	-3,74916
Druglikeness	ID	Value
	CMC_like_Rule	Qualified
	CMC_like_Rule_Violation_Fields	
	CMC_like_Rule_Violations	0
	Lead-like_Rule_Violation_Fields	
	Lead_like_Rule	Suitable if its binding affinity is greater than 0.1 microM
	Lead_like_Rule_Violations	0
	MDDR_like_Rule	Mid-structure
	MDDR_like_Rule_Violation_Fields	No_Rotatable_bonds
	MDDR_like_Rule_Violations	1
	Rule_of_Five	Suitable
	Rule_of_Five_Violation_Fields	
	Rule_of_Five_Violations	0
	WDI_like_Rule	In 90% cutoff
	WDI_like_Rule_Violation_Fields	
	WDI_like_Rule_Violations	0
Compound 10-3: Toxicity, ADME and Druglikeness		
Toxicity	ID	Value
	algae_at	0.115138
	Ames_test	mutagen
	Carcino_Mouse	negative
	Carcino_Rat	positive
	daphnia_at	0.691772
	hERG_inhibition	medium_risk
	medaka_at	0.889297
	minnow_at	0.812331

	TA100_10RLI	negative
	TA100_NA	negative
	TA1535_10RLI	positive
	TA1535_NA	negative
ADME	ID Value	
	BBB	0.0412772
	Buffer_solubility_mg_L	3287,97
	Caco2	15,0552
	CYP_2C19_inhibition	Non
	CYP_2C9_inhibition	Inhibitor
	CYP_2D6_inhibition	Non
	CYP_2D6_substrate	Non
	CYP_3A4_inhibition	Non
	CYP_3A4_substrate	Weakly
	HIA	58,758405
	MDCK	1,78554
	Pgp_inhibition	Non
	Plasma_Protein_Binding	65,960353
	Pure_water_solubility_mg_L	23,6455
	Skin_Permability	-4,94293
	SKlogD_value	0.683280
SKlogP_value	0.683280	
SKlogS_buffer	-2,02756	
SKlogS_pure	-4,17074	
Druglikeness	ID Value	
	CMC_like_Rule	Qualified
	CMC_like_Rule_Violation_Fields	
	CMC_like_Rule_Violations	0
	Lead-like_Rule_Violation_Fields	Molecular_weight, AlopP98_value
	Lead_like_Rule	Violated
	Lead_like_Rule_Violations	2
	MDDR_like_Rule	Mid-structure
	MDDR_like_Rule_Violation_Fields	No_Rotatable_bonds
	MDDR_like_Rule_Violations	1
	Rule_of_Five	Suitable
	Rule_of_Five_Violation_Fields	
	Rule_of_Five_Violations	0
	WDI_like_Rule	In 90% cutoff
	WDI_like_Rule_Violation_Fields	
	WDI_like_Rule_Violations	0

Conclusion

Our study presents a straightforward and efficient synthesis method for generating 1,3,4-oxadiazole and 1,3,4-bisoxadiazole derivatives featuring aromatic chain substituents. This method not only significantly reduces reaction time but also proves to be energy-efficient, yielding satisfactory product quantities. The synthesized compounds were validated through spectral data analysis,

including IR, ¹H NMR, and MS. Notably, our compounds exhibited promising results in ADMET, Docking, and molecular dynamics studies. Particularly noteworthy is the observation that the presence of heteroatoms and the structural geometry of the HIV protein significantly impact the binding affinity of the studied compounds to the active site. In this regard, compound 10-2 demonstrated a remarkable affinity of -7.5

kcal/mol for the HIV protein in Extra Precision mode (XP), while compound 10-3 exhibited -7.1 kcal/mol in Standard Precision mode. These findings underscore the potential of 1,3,4-oxadiazole and 1,3,4-bisoxadiazole compounds and warrant further exploration through future biological and chemical studies.

Declaration of Funding

The authors do not have financial support according to an institution

Conflicts of Interest

The authors declare no conflicts of interest.

References

1. Chandrakantha B, Shetty P, Nambiyar V, et al (2010) Synthesis, characterization and biological activity of some new 1,3,4-oxadiazole bearing 2-fluoro-4-methoxy phenyl moiety. *Eur J Med Chem* 45:1206–1210. <https://doi.org/10.1016/j.ejmech.2009.11.046>
2. Ahsan MJ, Choupra A, Sharma RK, et al (2018) Rationale Design, Synthesis, Cytotoxicity Evaluation, and Molecular Docking Studies of 1,3,4-oxadiazole Analogues. *Anti-Cancer Agents Med Chem- Anti-Cancer Agents* 18:121–138. <https://doi.org/10.2174/1871520617666170419124702>
3. Jadhav R, Pawar S, Khilare C, Nikumbh A (2023) Synthesis and biological screening of novel series of 2-(4-hydroxy-3-methoxy-5-nitrophenyl)-[1,3,4]oxadiazole by conventional and non conventional techniques. *Mater Today Proc* 73:487–493. <https://doi.org/10.1016/j.matpr.2022.10.087>
4. Reddy KK, Vidya Rajan VK, Gupta A, et al (2015) Exploration of binding site pattern in arachidonic acid metabolizing enzymes, Cyclooxygenases and Lipoxygenases. *BMC Res Notes* 8:152. <https://doi.org/10.1186/s13104-015-1101-4>
5. Siwach A, Verma PK (2020) Therapeutic potential of oxadiazole or furadiazole containing compounds. *BMC Chem* 14:70. <https://doi.org/10.1186/s13065-020-00721-2>
6. Li Y, Liu J, Zhang H, et al (2006) Stereoselective synthesis and fungicidal activities of (E)- α -(methoxyimino)-benzeneacetate derivatives containing 1,3,4-oxadiazole ring. *Bioorg Med Chem Lett* 16:2278–2282. <https://doi.org/10.1016/j.bmcl.2006.01.026>
7. Hamada NMM, Sharshira EM (2011) Synthesis and Antimicrobial Evaluation of Some Heterocyclic Chalcone Derivatives. *Molecules* 16:2304–2312. <https://doi.org/10.3390/molecules16032304>
8. Loetchutinat C, Chau F, Mankhetkorn S (2003) Synthesis and Evaluation of 5-Aryl-3-(4-hydroxyphenyl)-1,3,4-oxadiazole-2-(3H)-thiones as P-Glycoprotein Inhibitors. *Chem Pharm Bull (Tokyo)* 51:728–730. <https://doi.org/10.1248/cpb.51.728>
9. Abadi AH, Eissa AAH, Hassan GS (2003) Synthesis of Novel 1,3,4-Trisubstituted Pyrazole Derivatives and Their Evaluation as Antitumor and Antiangiogenic Agents. *Chem Pharm Bull (Tokyo)* 51:838–844. <https://doi.org/10.1248/cpb.51.838>
10. Kumar D, Sundaree S, Johnson EO, Shah K (2009) An efficient synthesis and biological study of novel indolyl-1,3,4-oxadiazoles as potent anticancer agents. *Bioorg Med Chem Lett* 19:4492–4494. <https://doi.org/10.1016/j.bmcl.2009.03.172>
11. Raman K, Singh HK, Salzman SK, Parmar SS (1993) Substituted thiosemicarbazides and corresponding cyclized 1,3,4-oxadiazoles and their anti-inflammatory activity. *J Pharm Sci* 82:167–169. <https://doi.org/10.1002/jps.2600820210>
12. Sahin G, Palaska E, Kelicen P, et al (2001) Synthesis of Some New 1-Acylthiosemicarbazides, 1,3,4-Oxadiazoles, 1,3,4-Thiadiazoles and 1,2,4-Triazole-3-thiones and their Anti-inflammatory Activities. *Arzneimittelforschung* 51:478–484. <https://doi.org/10.1055/s-0031-1300066>
13. Yale HL, Losee K (2002) 2-Amino-5-Substituted 1,3,4-Oxadiazoles and 5-Imino-2-Substituted Δ 2-1,3,4-Oxadiazolines. A Group of Novel Muscle Relaxants. In: *ACS Publ.* <https://pubs.acs.org/doi/pdf/10.1021/jm00322a007>. Accessed 20 Jul 2023
14. PARIKH K, JOSHI D (2014) Synthesis and evaluation of 2-(5-(aryl)-1,3,4-oxadiazol-2-ylthio)-N-(3-(trifluoromethyl)phenyl)acetamides and N-(4-chloro-3-fluorophenyl)-2-(5-(aryl)-1,3,4-oxadiazol-2-ylthio)acetamides as antimicrobial agents. *J Chem Sci* 126:827–835. <https://doi.org/10.1007/s12039-014-0625-9>

15. Palmer JT, Hirschbein BL, Cheung H, et al (2006) Keto-1,3,4-oxadiazoles as cathepsin K inhibitors. *Bioorg Med Chem Lett* 16:2909–2914. <https://doi.org/10.1016/j.bmcl.2006.03.001>
16. Kangani CO, Kelley DE, Day BW (2006) One pot direct synthesis of oxazolines, benzoxazoles, and oxadiazoles from carboxylic acids using the Deoxo-Fluor reagent. *Tetrahedron Lett* 47:6497–6499. <https://doi.org/10.1016/j.tetlet.2006.07.032>
17. Khan MTH, Choudhary MI, Khan KM, et al (2005) Structure–activity relationships of tyrosinase inhibitory combinatorial library of 2,5-disubstituted-1,3,4-oxadiazole analogues. *Bioorg Med Chem* 13:3385–3395. <https://doi.org/10.1016/j.bmc.2005.03.012>
18. Rochdi A, Kassou O, Dkhireche N, et al (2014) Inhibitive properties of 2,5-bis(*n*-methylphenyl)-1,3,4-oxadiazole and biocide on corrosion, biocorrosion and scaling controls of brass in simulated cooling water. *Corros Sci* 80:442–452. <https://doi.org/10.1016/j.corsci.2013.11.067>
19. Salassa G, Terenzi A (2019) Metal Complexes of Oxadiazole Ligands: An Overview. *Int J Mol Sci* 20:3483. <https://doi.org/10.3390/ijms20143483>
20. Phillips MA (1928) CCCXVII.—The formation of 2-substituted benzimidazoles. *J Chem Soc Resumed* 2393–2399. <https://doi.org/10.1039/JR9280002393>
21. Galal SA, Hegab KH, Kassab AS, et al (2009) New transition metal ion complexes with benzimidazole-5-carboxylic acid hydrazides with antitumor activity. *Eur J Med Chem* 44:1500–1508. <https://doi.org/10.1016/j.ejmech.2008.07.013>
22. Bregman H, Chakka N, DiMauro EF, et al (2017) Biaryl acyl-sulfonamide compounds as sodium channel inhibitors
23. Farshori NN, Rauf A, Siddiqui MA, et al (2017) A facile one-pot synthesis of novel 2,5-disubstituted-1,3,4-oxadiazoles under conventional and microwave conditions and evaluation of their in vitro antimicrobial activities. *Arab J Chem* 10:S2853–S2861. <https://doi.org/10.1016/j.arabjc.2013.11.010>
24. Jewel PW, Butts JS (2002) A Method for the Preparation of Diethyl Oxalate. In: ACS Publ. <https://pubs.acs.org/doi/pdf/10.1021/ja01360a052>. Accessed 20 Jul 2023
25. Fayed EA, Ammar YA, Saleh MA, et al (2021) Design, synthesis, antiproliferative evaluation, and molecular docking study of new quinoxaline derivatives as apoptotic inducers and EGFR inhibitors. *J Mol Struct* 1236:130317. <https://doi.org/10.1016/j.molstruc.2021.130317>
26. Hendrickson JB, Hussoin MS (2002) Reactions of carboxylic acids with phosphonium anhydrides. In: ACS Publ. <https://pubs.acs.org/doi/pdf/10.1021/jo00266a028>. Accessed 20 Jul 2023
27. Kaul S, Kumar A, Sain B, Bhatnagar AK (2007) Simple and Convenient One-Pot Synthesis of Benzimidazoles and Benzoxazoles using *N,N*-Dimethylchlorosulfitemethaniminium Chloride as Condensing Agent. *Synth Commun* 37:2457–2460. <https://doi.org/10.1080/00397910701459423>
28. I.M. Labouta, A.M.M. Hassan, O.M. Aboulwafa, O. Kader, Synthesis of some substituted benzimidazoles with potential antimicrobial activity, *Monatsh. Chem.* 120 (6–7) (1989) 571–574.
29. MarcinLuczynski and AgnieszkaKudelko, Synthesis and Biological Activity of 1,3,4-Oxadiazoles Used in Medicine and Agriculture, *Appl.Sci.* 2022, **12(8)**,3756; <https://doi.org/10.3390/app12083756>